# Interference-Aided Detection of Subthreshold Signal Using Beam Control in Polarization Diversity Reception

Shintaro Hiraoka, *Student Member, IEEE,* Yasuo Nakashima, *Student Member, IEEE,* Takaya Yamazato, *Senior Member, IEEE,* Shintaro Arai, *Member, IEEE,* Yukihiro Tadokoro, *Member, IEEE,* Hiroya Tanaka, *Senior Member, IEEE,*

***Abstract*—The present article discusses a detectability enhancement induced by co-channel interference signals in the polarization diversity reception. The challenge is the detection of weak (subthreshold) signals, the level of which is less than the detection limit of radio receivers. To understand the theory underlying the mechanism in the presented diversity scheme, we introduce an analytic model of a dual polarized antenna array in the fading channel. In addition, the channel capacity in a binary data transmission is derived. As a result, we reveal that the interference-aided diversity reception enables us to detect signals even below the detection limit of the receiver. Moreover, appropriate source code is needed to achieve the channel capacity because the transmission channel is asymmetric in the present reception scheme.**

***Index Terms*—Polarization diversity, subthreshold, weak signal detection, channel capacity, stochastic resonance.**

## I. Introduction

In wireless communications, signals are degraded during propagation due to fading and co-channel interference [1], [2]. Diversity reception compensates for such degradation, and several kinds of reception have been analytically and experimentally demonstrated for time, frequency, and space diversities [3]. In space diversity, a signal sent over different uncorrelated paths is received using multiple antennas. Space diversity reception has been investigated in mobile communications, such as a body area network [4] and relay networks [5], [6]. Such diversity reception leads to a great enhancement in terms of the communication performance, e.g., signal-to-noise ratio, channel capacity, and throughput.

Stochastic resonance (SR) enhances the detectability of weak (subthreshold) signals by transduction via a nonlinear element [7]. The concept of SR has potential applications in computing [8] and imaging [9]. In particular, much effort has been devoted to the investigation of weak signal detection in communication systems [10]–[12]. For example, in [10], SR was discussed in cognitive radios, and signals were successfully detected with a SR-based sequential sensing scheme. In [11], a stochastic resonator has been proposed. The bit-error ratio was improved in the binary data transmission of the pulse amplitude modulated signal by tuning the parameters of the bistable system. In [12], the band-limiting filter has been demonstrated. The bit-error was reduced by a root-raised-cosine filter in the receiver with SR. However, to the best of our knowledge, diversity reception based on SR has not been investigated.

In this letter, we extend the concept of SR to diversity reception to detect subthreshold signals below the detection limit of the receiver. A significant improvement in the signal detectability is demonstrated by introducing interference-aided detection in the polarization diversity. To evaluate the functionality of the interference-aided detection, a simple propagation scenario described by a fading model is considered. The channel capacity in a binary data transmission is then derived. Throughout the analysis, we reveal that an appropriate source coding should be applied to achieve the channel capacity because the transmission channel is asymmetric in the proposed diversity reception.

It should be noted that the proposed scheme is completely different from the conventional space diversity approach. The conventional space diversity controls the combining weights to increase the diversity gain; i.e., it suppresses the co-channel interference signals, which inherently degrades the reception of the desired signal. In contrast, the proposed approach uses the interference signals to improve the communication performance. In addition, the interference signals allow the detection of signals below the detection limit of the radio receiver.

## II. Performance analysis

### A. System configuration

We study the detectability enhancement induced by co-channel interference signals in the polarization diversity reception as shown in Fig. 1(a). A binary channel input for the on-off-keying modulation is considered. The system consists of horizontally and vertically polarized antenna arrays, combiners, weight multipliers, and a two-level quantizer. The signals received by the antennas are weighted and then combined. The signal $r = r_{\mathrm{h}} + r_{\mathrm{v}}$ is the output at the frontend of the antenna array, where $r_{\mathrm{h}}$ and $r_{\mathrm{v}}$ are the received signals at the horizontally and vertically polarized antenna arrays,

S. Hiraoka, Y. Nakashima and T. Yamazato are with Nagoya University, Nagoya 464-8603, Japan (e-mail: hiraoka@katayama.nuee.nagoya-u.ac.jp, nakasima@katayama.nuee.nagoya-u.ac.jp, and yamazato@nagoya-u.jp).

S. Arai is with Okayama University of Science, Okayama 700-0005, Japan (e-mail: arai@ee.ous.ac.jp).

Y. Tadokoro and H. Tanaka are with Toyota Central R&D Laboratories, Inc., Aichi 480-1192, Japan (e-mail: y.tadokoro@ieee.org, and tanak@mosk.tytlabs.co.jp).

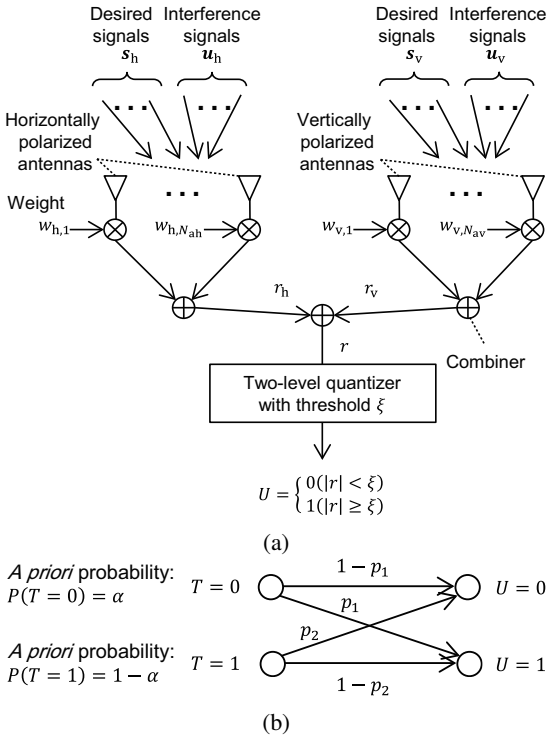


Fig. 1: (a) Schematic depiction of the interference-aided signal detection in the polarization diversity. (b) Binary asymmetric channel. Channel transition probabilities are expressed as $P(U = 1|T = 0) = p_1$ and $P(U = 0|T = 1) = p_2$.

respectively. The two-level quantizer has a given threshold $\xi$, which is assumed to be the detection limit of the receiver. More specifically, the subthreshold signals $|r| < \xi$ cannot be identified by the receiver. Considering the binary signal input to the quantizer, the output symbol $U$ at the system frontend is expressed as

$$U = \begin{cases} 0, & \text{for } |r| < \xi \\ 1, & \text{for } |r| \geq \xi \end{cases} . \tag{1}$$

Significantly, the subthreshold signal is detectable via the nonlinear signal processing, i.e., the two-level quantization of the signal $r$, due to SR [7]–[12].

### B. Analytic model

The output of the arrays is

$$\begin{aligned} r &= r_h + r_v \\ &= \begin{bmatrix} \boldsymbol{g}_{sh}^T & \boldsymbol{g}_{uh}^T \end{bmatrix} \begin{bmatrix} \boldsymbol{s}_h \\ \boldsymbol{u}_h \end{bmatrix} + \begin{bmatrix} \boldsymbol{g}_{sv}^T & \boldsymbol{g}_{uv}^T \end{bmatrix} \begin{bmatrix} \boldsymbol{s}_v \\ \boldsymbol{u}_v \end{bmatrix}, \end{aligned} \tag{2}$$

where $\boldsymbol{s}_h = [s_{h,1}, \cdots, s_{h,N_{sh}}]^T$ and $\boldsymbol{u}_h = [u_{h,1}, \cdots, u_{h,N_{uh}}]^T$ ($\boldsymbol{s}_v = [s_{v,1}, \cdots, s_{v,N_{sv}}]^T$ and $\boldsymbol{u}_v = [u_{v,1}, \cdots, u_{v,N_{uv}}]^T$) are the vectors of the desired and interference signals of the horizontal (vertical) component, respectively. Such signals are weighted with the angular sensitivity of the arrays $\boldsymbol{g}_{sh} = [g_{sh,1}, \cdots, g_{sh,N_{sh}}]^T$ and $\boldsymbol{g}_{uh} = [g_{uh,1}, \cdots, g_{uh,N_{uh}}]^T$ ($\boldsymbol{g}_{sv} = [g_{sv,1}, \cdots, g_{sv,N_{sv}}]^T$ and $\boldsymbol{g}_{uv} = [g_{uv,1}, \cdots, g_{uv,N_{uv}}]^T$), which are determined by the weight vectors $w_h = [w_{h,1}, \cdots, w_{h,N_{ah}}]^T$ ($w_v = [w_{v,1}, \cdots, w_{v,N_{av}}]^T$). The parameters $N_{sh}$ and $N_{sv}$, $N_{uh}$ and $N_{uv}$, and $N_{ah}$ and $N_{av}$ are the numbers of desired signals, the numbers of interference signals, and the numbers of antennas in the arrays, respectively. Here, the subscripts "h" and "v" refer to the horizontal and vertical polarizations, respectively, and $\boldsymbol{y}^T$ denotes the transpose of the vector $\boldsymbol{y}$.

To identify the underlying mechanism for the interference-aided detection, it is assumed that $\boldsymbol{s}_h = [s_0(< \xi)]$ and $\boldsymbol{s}_v = \boldsymbol{0}$, i.e., the single desired signal is received at the horizontally polarized antennas and not at the vertical antennas. Moreover, a multipath fading channel model is used for the interference signal propagation; i.e., the interference signals arrive at the receiver with equal magnitudes and random phases. The signals $r_h$ and $r_v$ are then expressed as

$$r_h = s_0 + \sum_{n_h=1}^{N_{uh}} a_{h,n_h} e^{j\phi_{h,n_h}}, \tag{3a}$$

$$r_v = g \sum_{n_v=1}^{N_{uv}} a_{v,n_v} e^{j\phi_{v,n_v}}, \tag{3b}$$

where $a_{h,n_h}$ and $a_{v,n_v}$ are the magnitudes, and $\phi_{h,n_h}$ and $\phi_{v,n_v}$ are the phases of the interference signals. In (3b), it is assumed that all of the signals are combined with equal gains at each polarized antenna array, i.e., $g_{sh,1} = g_{uh,1} = \cdots = g_{uh,N_{uh}} = g_h$ and $g_{uv,1} = \cdots = g_{uv,N_{uv}} = g_v$, $g = g_v/g_h$ with $g_h = 1$. Note that the angular sensitivity is designed via signal processing, such as beamforming, in practical implementations. However, in the present study, the angular sensitivity should be tuned in the range of $0 \leq g \leq 1$ to obtain the best performance in the proposed system.

Specifically, (3a) includes a line-of-sight path (first term of the right-hand side) and the other paths (second term of the right-hand side). This is modeled as the Rician fading channel. The probability density functions (PDFs) of the in-phase and quadrature components are expressed as Gaussian distributions $N(s_0, \sigma_h^2)$ and $N(0, \sigma_h^2)$. Moreover, (3b) is expressed as multiple paths without the dominant path. This is modeled as the Rayleigh fading channel. The PDFs of the in-phase and quadrature components are expressed as $N(0, g^2\sigma_v^2)$ and $N(0, g^2\sigma_v^2)$. Note that $\sigma_h^2$ and $\sigma_v^2$ are the variances of the interference signals received at the horizontally and vertically polarized antenna arrays.

Considering the joint probability, the PDFs of the in-phase and quadrature components of the signal $r$ are written as $f_I = N(s_0, \sigma_h^2) * N(0, g^2\sigma_v^2)$ and $f_Q = N(0, \sigma_h^2) * N(0, g^2\sigma_v^2)$, respectively. Note that the operation denoted by $N_h * N_v$ is the convolution of the PDFs $N_h$ and $N_v$. According to the transformation of random variables and the marginal probability, the PDF of the magnitude of the signal $r$ is described as

$$f_a(a|s_0, \sigma_h^2, g\sigma_v^2) = \int_0^{2\pi} f_{a\phi}(a, \phi) \mathrm{d}\phi, \tag{4}$$

where $f_{a\phi} = f_I f_Q |J|$, $|J|$ is the Jacobian matrix, $a = |r|$, and $\phi = \arg(r)$. Based on (4), the PDF $f_a$ is manipulated by the sensitivity $g$.

For the purpose of clarification, a simplistic situation with the specific variables $\phi_{h,1} = \cdots = \phi_{h,N_h} = 0$ and $\phi_{v,1} = \cdots = \phi_{v,N_v} = 0$ was deliberately considered. This toy model helps us to understand the mechanism of the interference-aided

detection. The condition $|r| < \xi$ in (1) is rewritten as $s_0 < \xi - b$ where $b = N_{\rm uh}a_{\rm h,1} + gN_{\rm uv}a_{\rm v,1}$. The bias term $b$ decreases the detection limit $\xi$ via SR [7]–[12]. To obtain an effective signal enhancement based on SR, the magnitude of $b$ is tuned by the sensitivity $g$. Therefore, the interference signals enable the detection of the subthreshold signal in the polarization diversity reception.

### C. Channel capacity

To investigate the performance of the interference-aided detection, the channel capacity is analytically derived. The transmission channel is illustrated in Fig. 1(b). The channel capacity is given as the maximum of the mutual information $I(T;U) = H(U) - H(U|T)$, where $T = \{0,1\}$ is a random variable representing the channel input, and the operator $H(\cdot)$ provides the entropy of a memoryless source. Let us consider *a priori* probabilities $P(T=0) = \alpha$ and $P(T=1) = 1-\alpha$. According to (4), the channel transition probabilities are expressed as $P(U=1|T=0) = p_1 = \int_{\xi}^{\infty} f_{\rm a}(a|s_0=0){\rm d}a$ and $P(U=0|T=1) = p_2 = \int_{0}^{\xi} f_{\rm a}(a|s_0=1){\rm d}a$.

Considering ${\rm d}[I(T;U)]/{\rm d}\alpha = 0$, the channel capacity is derived as [13]

$$c = \log_2\left(1 + 2^{\frac{h(p_1)-h(p_2)}{1-p_1-p_2}}\right) + \frac{1-p_2}{1-p_1-p_2}h(p_1) + \frac{p_1}{1-p_1-p_2}h(p_2), \tag{5a}$$

at the *a priori* probability,

$$\alpha = \frac{1-p_2\left(1+2^{\frac{h(p_1)-h(p_2)}{1-p_1-p_2}}\right)}{\left(1+2^{\frac{h(p_1)-h(p_2)}{1-p_1-p_2}}\right)(1-p_1-p_2)}, \tag{5b}$$

where $h(p) = -p\log_2 p - (1-p)\log_2(1-p)$.

## III. Performance result

Figure 2(a) shows a map of the channel capacity. The channel capacity is observed to vary as a function of the sensitivity $g$ and the threshold $\xi$. To better understand the relationship among them, the channel capacities are plotted for several values of the sensitivity $g$ in Fig. 2(b), i.e., the channel capacities along the pink dotted lines in Fig. 2(a). The peaks of the channel capacities $c = 0.2$, 0.1, and 0.05 bits are observed at $(\xi, g) = (1.2, 0.20)$, $(1.5, 0.41)$, and $(1.8, 0.55)$, respectively. This indicates that the sensitivity $g$ should be appropriately adjusted to obtain the best performance for a given threshold $\xi$, which depends on the specifications of the receivers.

In addition, there exist local maxima of the channel capacity in the dimension of the threshold $\xi$. Specifically, the local maxima can be seen on a ridge, which is represented by the white dashed line in Fig. 2(a). Figure 2(c) shows the local maxima of the channel capacity along the ridge line in Fig. 2(a). A maximum capacity of 0.2 bits is observed at $\xi = 1.2$, which is the lower limit for the range of values considered herein, $1.2 \le \xi \le 2.8$. The channel capacity decreases monotonically with the threshold because the enhancement based on SR is inversely proportional to the threshold level of the quantizer [7].

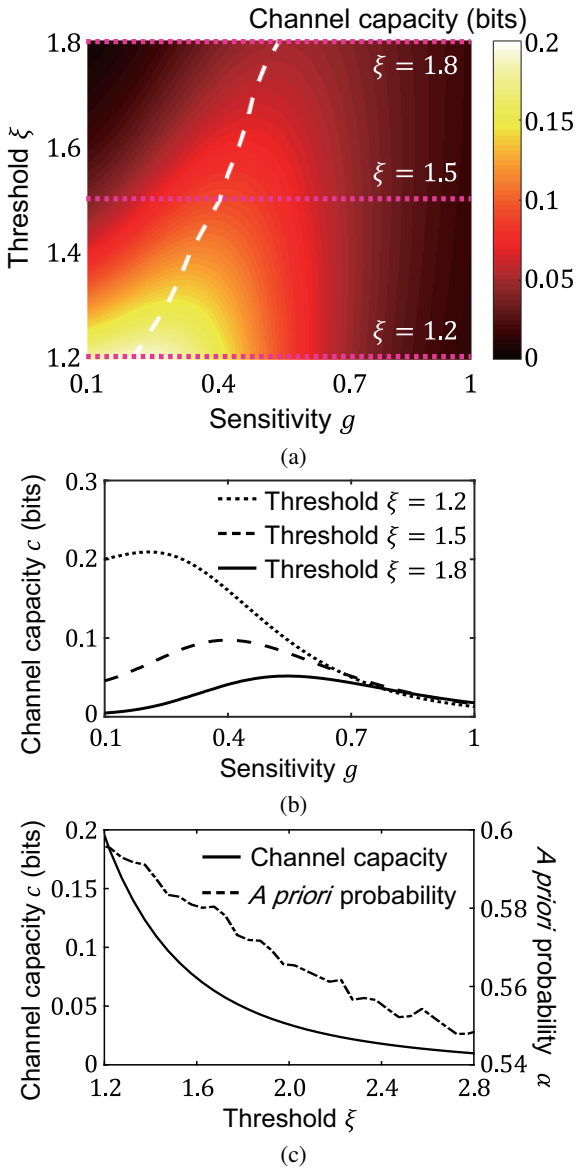


Fig. 2: (a) Channel capacity. Local maxima of the capacity in the dimension of the quantizer threshold $\xi$ are shown by the white dashed line. (b) Channel capacities for the specific thresholds $\xi = 1.2$, 1.5 and 1.8. (c) Channel capacity and *a priori* probability on the ridge line in (a). The parameter settings are $s_0 = \{0,1\}$, $\sigma_{\rm v}^2 = 1$, and $\sigma_{\rm h}^2 = 0.09$.

Moreover, the channel capacity can be described as a function of the *a priori* probability $\alpha$ as (5b). Figure 2(c) also shows the *a priori* probability providing the channel capacity on the ridge line in Fig. 2(a). This means that an appropriate encoding scheme for the channel input $T$ is necessary for the transmitter to achieve a high throughput that is close to the channel capacity in practical implementations.

To further investigate the system behavior, the PDFs of the signal magnitude are plotted for $f_{\rm a}(a|s_0=0)$ and $f_{\rm a}(a|s_0=1)$ in Figs. 3(a) and 3(b), respectively. Comparing Figs. 3(a) and 3(b), it can be clearly seen that the PDFs vary with the presence of the desired signal $s_0$. Moreover, the PDF changes drastically with the sensitivity $g$. To capture the channel

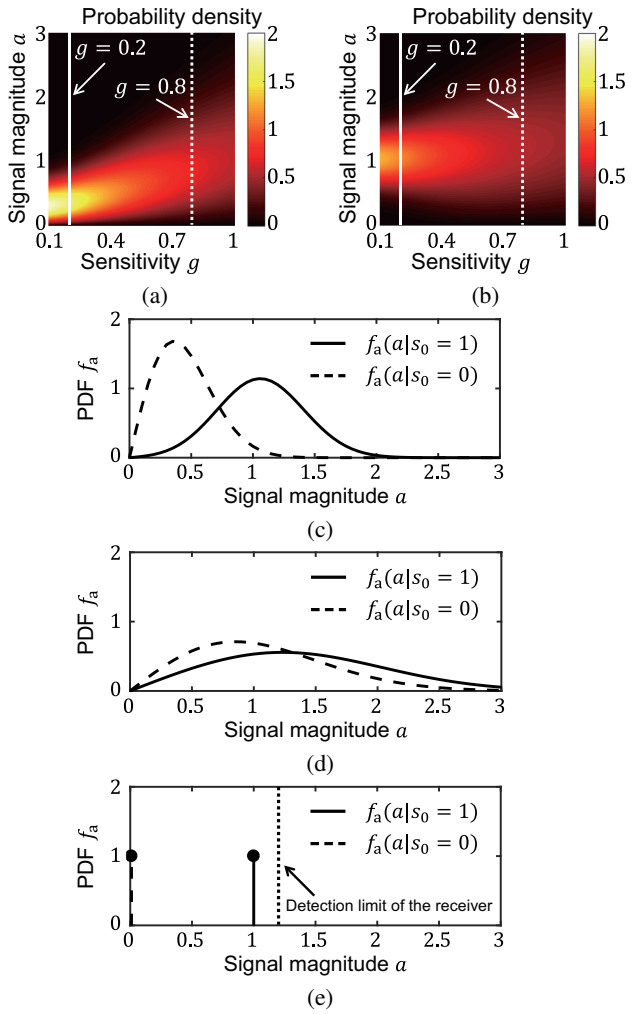


Fig. 3: PDFs of the signal magnitude $a$ in the cases of (a) $s_0 = 1$ and (b) $s_0 = 0$. PDFs of the signal amplitude $a$ in the cases of (c) $g = 0.2$ and (d) $g = 0.8$, which are along the white solid and dotted lines in both (a) and (b). The parameter settings are $\sigma_v^2 = 1$ and $\sigma_h^2 = 0.09$ in (a) to (d). (e) PDF of the signal magnitude $a$ for the case without interference, i.e., $\sigma_v^2 = \sigma_h^2 = 0$. The detection limit $\xi_{\min} = 1.2$ is shown by the dotted line in (e).

variation with the sensitivity, PDFs for $g = 0.2$ and 0.8 are plotted in Figs. 3(c) and 3(d), which are obtained along the white solid and dotted lines in Figs. 3(a) and 3(b). In Fig. 3(c), a distinct discrepancy is observed between the PDFs for the cases with the signal $s_0$ (solid line) and without the signal $s_0$ (dashed line). This indicates that the symbols, 0 or 1, can be identified via the two-level quantization. In Fig. 3(d), on the other hand, there is a small variation between the cases of $s_0 = 1$ (solid line) and $s_0 = 0$ (dashed line). The situation shown in Fig. 3(d) presents a lower detectability than Fig. 3(c).

Finally, we should point out that the subthreshold signal is not detectable when there is no interference signal. To see this, the PDFs $f_a(a|s_0 = 0)$ and $f_a(a|s_0 = 1)$ for $\sigma_h^2 = \sigma_v^2 = 0$ are plotted in Fig. 3(e). The receiver outputs only zero, i.e., $U = 0$, for the case in which the magnitude of the desired signal is less than the detection limit, i.e., $s_0 < \xi$; for instance, the limit is equal to 1.2, as shown by the dotted line. This implies that the subthreshold signal is not entirely detectable, i.e., $c = 0$, in the traditional space diversity reception, which does not amplify the signals [3]. In contrast, the interference signals bring the PDF $f_a(a|s_0 = 1)$ into the detectable region ($> \xi = 1.2$), as shown in Figs. 3(c) and 3(d). As such, these interference signals allow the detection of the subthreshold signal due to the amplification of the desired signal. This means that the interference-aided detection provides a breakthrough in severe scenarios in which the desired signal cannot be detected by the conventional reception scheme.

## IV. Conclusion

In the present study, a scheme for interference-aided detection in polarization diversity reception was proposed. In this scheme, the detectability of the subthreshold signal was dramatically improved through nonlinear signal processing by stochastic resonance. To elaborate the performance of the interference-aided detection, we analytically derived the channel capacity for the binary asymmetric data transmission. As a result, a capacity of 0.2 bits was obtained with an appropriate beam control of the dual-polarized antenna arrays. In addition, a proper source coding enables us to obtain the channel capacity. The interference-aided detection will be extended to other modulation schemes to be dealt with in future publications.

## Acknowledgment

The authors would like to thank Prof. Masaaki Katayama, associate Prof. Hiraku Okada, and assistant Prof. Kentaro Kobayashi for their fruitful discussions.

## References

[1] W. C. Jakes, *Microwave Mobile Communications*. New York, NY, USA: Wiley, 1974.
[2] T. S. Rappaport, *Wireless Communications: Principles and Practice*, 2nd ed. Upper Saddle River, NJ, USA: Prentice Hall, 2002.
[3] A. Goldsmith, *Wireless Communications*. Cambridge, U.K.: Cambridge Univ. Press, 2005.
[4] P.-F. Cui, W.-J. Lu, Y. Yu, B. Xue, and H.-B. Zhu, "Off-body spatial diversity reception using circular and linear polarization: measurement and modeling," *IEEE Commun. Lett.*, vol. 22, pp. 209–212, 2018.
[5] E. Erdogan, A. Afana, T. Gucluoglu, and S. Ikki, "Unified analysis and optimization study of antenna selection in two-way relay networks," *IEEE Wireless Commun. Lett.*, vol. 5, pp. 216–219, 2016.
[6] E. Erdogan, A. Afana, S. Ikki, and H. Yanikomeroglu, "Antenna selection in MIMO cognitive af relay networks with mutual interference and limited feedback," *IEEE Commun. Lett.*, vol. 21, pp. 1111–1114, 2017.
[7] R. Benzi, A. Sutera, and A. Vulpiani, "The mechanism of stochastic resonance," *J. Phys. A, Math. Gen.*, vol. 14, pp. L453–L457, 1981.
[8] J. Teramae and T. Fukai, "Computational implications of lognormally distributed synaptic weights," *Proc. IEEE*, vol. 102, pp. 500–512, 2014.
[9] H. Chen, L. R. Varshney, and P. K. Varshney, "Noise-enhanced information systems," *Proc. IEEE*, vol. 102, pp. 1607–1621, 2014.
[10] Q. Li and Z. Li, "A novel sequential spectrum sensing method in cognitive radio using suprathreshold stochastic resonance," *IEEE Trans. Veh. Technol.*, vol. 63, pp. 1717–1725, 2014.
[11] J. Liu, Z. Li, L. Guan, and L. Pan, "A novel parameter-tuned stochastic resonator for binary PAM signal processing at low SNR," *IEEE Commun. Lett.*, vol. 18, pp. 427–430, 2014.
[12] Y. Nakashima, H. Tanaka, T. Yamazato, Y. Tadokoro, and S. Arai, "Effect of a root-raised-cosine filter on a BPSK stochastic resonance receiver," *NOLTA, IEICE*, vol. 8, pp. 204–214, 2017.
[13] F. Chapeau-Blondeau, "Noise-enhanced capacity via stochastic resonance in an asymmetric binary channel," *Phys. Rev. E.*, vol. 55, pp. 2016–2019, 1997.